the plant journal

SEB SOCIETY FOR EXPERIMENTAL BIOLOGY

The Plant Journal (2022) **112,** 309–321 doi: 10.1111/tpj.15962

FRIENDLY (FMT) is an RNA binding protein associated with cytosolic ribosomes at the mitochondrial surface

Mickaele Hemono[1] , Thalia Salinas-Giegé[1] , Jeanne Roignant[1] , Audrey Vingadassalon[1,2] , Philippe Hammann[3] , Elodie Ubrig[1] , Patryk Ngondo[1,4] and Anne-Marie Duchêne[1,*]

[1]*Institut de biologie moléculaire des plantes, UPR 2357 du CNRS, Université de Strasbourg, 12 rue du Général Zimmer, 67084, Strasbourg Cedex, France,*

[2]*Université des Antilles, COVACHIM M2E (EA 3592), UFR SEN, Campus de Fouillole, F-97 110, Pointe-à-Pitre, France,*

[3]*Plateforme Protéomique Strasbourg-Esplanade, Institut de Biologie Moléculaire et Cellulaire, FR1589 du CNRS, 2 Allée Konrad Roentgen, 67084, Strasbourg Cedex, France, and*

[4]*Institut de Biologie Moléculaire et Cellulaire, UPR 9002 du CNRS, Université de Strasbourg, 2 Allée Konrad Roentgen, 67 084, Strasbourg Cedex, France*

Received 8 February 2022; revised 22 July 2022; accepted 15 August 2022; published online 1 September 2022.
*For correspondence (e-mail anne-marie.duchene@ibmp-cnrs.unistra.fr)

SUMMARY

The spatial organization of protein synthesis in the eukaryotic cell is essential for maintaining the integrity of the proteome and the functioning of the cell. Translation on free polysomes or on ribosomes associated with the endoplasmic reticulum has been studied for a long time. More recent data have revealed selective translation of mRNAs in other compartments, in particular at the surface of mitochondria. Although these processes have been described in many organisms, particularky in plants, the mRNA targeting and localized translation mechanisms remain poorly understood. Here, the *Arabidopsis thaliana* Friendly (FMT) protein is shown to be a cytosolic RNA binding protein that associates with cytosolic ribosomes at the surface of mitochondria. FMT knockout delays seedling development and causes mitochondrial clustering. The mutation also disrupts the mitochondrial proteome, as well as the localization of nuclear transcripts encoding mitochondrial proteins at the surface of mitochondria. These data indicate that FMT participates in the localization of mRNAs and their translation at the surface of mitochondria.

Keywords: mRNA trafficking, localized translation, co-translational import.

Linked article: This paper is the subject of a Research Highlight article. To view this Research Highlight article visit https://doi.org/10.1111/tpj.15992.

INTRODUCTION

Mitochondria are vital organelles for the eukaryotic cell, through their roles in ATP synthesis and other metabolic pathways. Their biogenesis is not only based on the expression of the mitochondrial genome, but also relies on a massive import of nuclear-encoded proteins, which are translated in the cytosol. It has been recently shown that protein import can occur post-translationally and co-translationally. In accordance, cytosolic mRNAs and ribosomes were found to be associated with the mitochondrial surface in numerous organisms.

One-third to one-half of mRNAs coding for nuclear-encoded mitochondrial proteins were found at the surface of mitochondria in plants (Vincent et al., 2017), yeast (Saint-Georges et al., 2008; Williams et al., 2014) or mammals (Fazal et al., 2019). The mechanisms governing mRNAs targeting to the mitochondrial surface are poorly understood. Both nucleotide motifs in the transcript and sequence signals in the newly synthesized protein can be important for mitochondrial surface localization of mRNAs (Lashkevich & Dmitriev, 2021; Lesnik et al., 2015).

Cytosolic ribosomes near the mitochondrial outer membrane were observed in yeast by Kellems et al. (1974) and were confirmed more recently by electron cryo-tomography (Gold et al., 2017). The precise mechanism of cytosolic ribosomes recruitment at the surface of mitochondria is not clear, although nascent polypeptide associated complex (Funfschilling & Rospert, 1999) and mitochondrial outer membrane protein OM14 (Lesnik et al., 2014) were shown involved in yeast, as well as the translocase of the outer membrane (TOM) complex

through the interaction with the targeting sequence of the newly synthesized protein (Gold et al., 2017).

Some RNA-binding proteins (RBPs) were found to be involved in mRNA localization and translation at the mitochondrial surface, such as PUF3 in yeast (Saint-Georges et al., 2008) or Larp in *Drosophila* (Zhang et al., 2016). The human CLUH was also shown to interact with mRNAs coding for mitochondrial proteins (Gao et al., 2014) and its *Drosophila* orthologue, Clueless, was able to bind ribosomal components at the surface of mitochondria (Sen & Cox, 2016). More recently, the CLUH interactome revealed the proximity of CLUH with mitochondrial proteins and their mRNAs during cytosolic translation (Hemono et al., 2022). CLUH and Clueless belong to the CLU family, which is widespread in all eukaryotes. CLU stands for 'CLUstered mitochondria' because knockdown of CLU proteins induces clustering of mitochondria in all organisms that have been investigated (El Zawily et al., 2014).

In plants, the specificities of cytosolic ribosomes at the surface of mitochondria are not known. Moreover, no RBP involved in mRNA localization and localized translation has been identified. To characterize ribosomes at the surface of the plant mitochondria, we have purified cytosolic ribosomes from an *Arabidopsis thaliana* mitochondrial extract. We have found that Friendly (FMT), the *A. thaliana* CLUH orthologue, was specifically enriched in this ribosomal fraction.

FMT has been previously identified using a microscopy-based screen to detect *A. thaliana* ethyl methanesulfonate (EMS) mutants with disrupted chondriome structure (Logan et al., 2003). In one of these mutants, mitochondria appeared to be either isolated or in large clusters of approximately 10 organelles. The involved mutation was localized in AT3G52140 locus, and the encoded protein was called FRIENDLY or FMT (Logan et al., 2003). FMT was subsequently shown to play a role in mediating inter-mitochondrial association and could be involved in regulating the mitochondrial fusion/fission balance (El Zawily et al., 2014).

Using reverse co-immunoprecipitation and split GFP approaches, we have confirmed our first result, comprising the association of FMT with the cytosolic ribosome and with the mitochondrial surface. We have also established that FMT is an RBP. At the level of mitochondria, the *fmt* knockout (KO) mutation was found to affect the mitochondrial proteome and the association of cytosolic mRNAs with mitochondria, suggesting a role of FMT in mRNA localization at the mitochondrial surface.

RESULTS

FMT copurifies with cytosolic ribosomes isolated from mitochondrial extracts

To characterize particular components of the cytosolic ribosome at the mitochondrial surface, an *A. thaliana* (*At*) line expressing an epitope-tagged cytosolic ribosomal protein, FLAG-RPL18 (AT3G05590), was used (Zanetti et al., 2005). Total and mitochondrial proteins extracts were prepared from FLAG-RPL18 and wild-type (Col0) inflorescences. Inflorescences were chosen because they are mitochondria-enriched tissues (Welchen et al., 2014). The quality of mitochondrial extracts was verified via Western blotting (Figure S1). Proteins were then immunoprecipitated with anti-FLAG beads (IP) and identified by LC–MS/MS analyses, and then spectral count label-free quantifications were performed. First, the IP with mitochondrial extracts were compared, that is IP with FLAG-RPL18 mitochondria (Rm-IP) and with Col0 mitochondria (Cm-IP) (Figure 1a), and 185 proteins were found enriched in Rm-IP [with cuts-off of fold change (FC) above 2 and adjusted *p* value (adj *p*) below 0.1]. One hundred and eleven out of the 185 proteins were from the cytosolic ribosome, confirming the presence of cytosolic ribosomes in the mitochondrial extract. IP from mitochondrial and total extracts from the FLAG-RPL18 line were also compared (Rm-IP versus Rt-IP, Figure 1b) and 96 proteins were found enriched in Rm-IP.

Sixty-three proteins appeared shared between the two comparisons, that is enriched in Rm-IP compared to both Cm-IP and Rt-IP (Figure 1c,d, Table S1). Five out of these 63 proteins have been identified as components of the cytosolic ribosome (Salih et al., 2020). Twenty-three others were annotated as mitochondrial according to SUBA4 (Hooper et al., 2017). No proteins from TOM complex were found, and only one protein from the mitochondrial outer membrane (MOM), the voltage-dependent anion channel VDAC2, was identified. This contrasts with results in yeast

Figure 1. Identification of proteins co-purifying with FLAG-RPL18 at the surface of mitochondria.
(a) FLAG-RPL18 mitochondrial coIP compared to the Col0 mitochondrial coIP (Rm-IP versus Cm-IP).
Immunoprecipitated proteins were identified by LC–MS/MS. Statistical analyses based on specific spectral counts identified 185 proteins enriched in Rm-IP compared to Cm-IP with cuts-off of FC above 2 and adj *p* below 0.1.
(b) FLAG-RPL18 mitochondrial coIP compared to FLAG-RPL18 total coIP (Rm-IP versus Rt-IP).
With the same cuts-off as in (a), 96 proteins were enriched in Rm-IP compared to Rt-IP.
In (a) and (b), the yellow spots correspond to the RPL18 bait. Proteins from cytosolic ribosomes (Salih et al., 2020) are shown in black. The 63 enriched proteins (c) are indicated by a red circle. FMT is shown in green.
(c) Sixty-three enriched proteins are shared in these two comparisons, Rm-IP versus Cm-IP (a) and Rm-IP versus Rt-IP (b).
(d) Graphs in (a) and (b) are enlarged for the 63 proteins. Five out of the 63 proteins are from the cytosolic ribosome (black). Among mitochondrial proteins, five are components of the mitochondrial membranes (green) and 10 are from the mitochondrial ribosome (blue). Mitochondrial ribosomes are known to be associated with membranes (Tomal et al., 2019; Waltz & Giege, 2020). The other mitochondrial proteins are shown in orange.

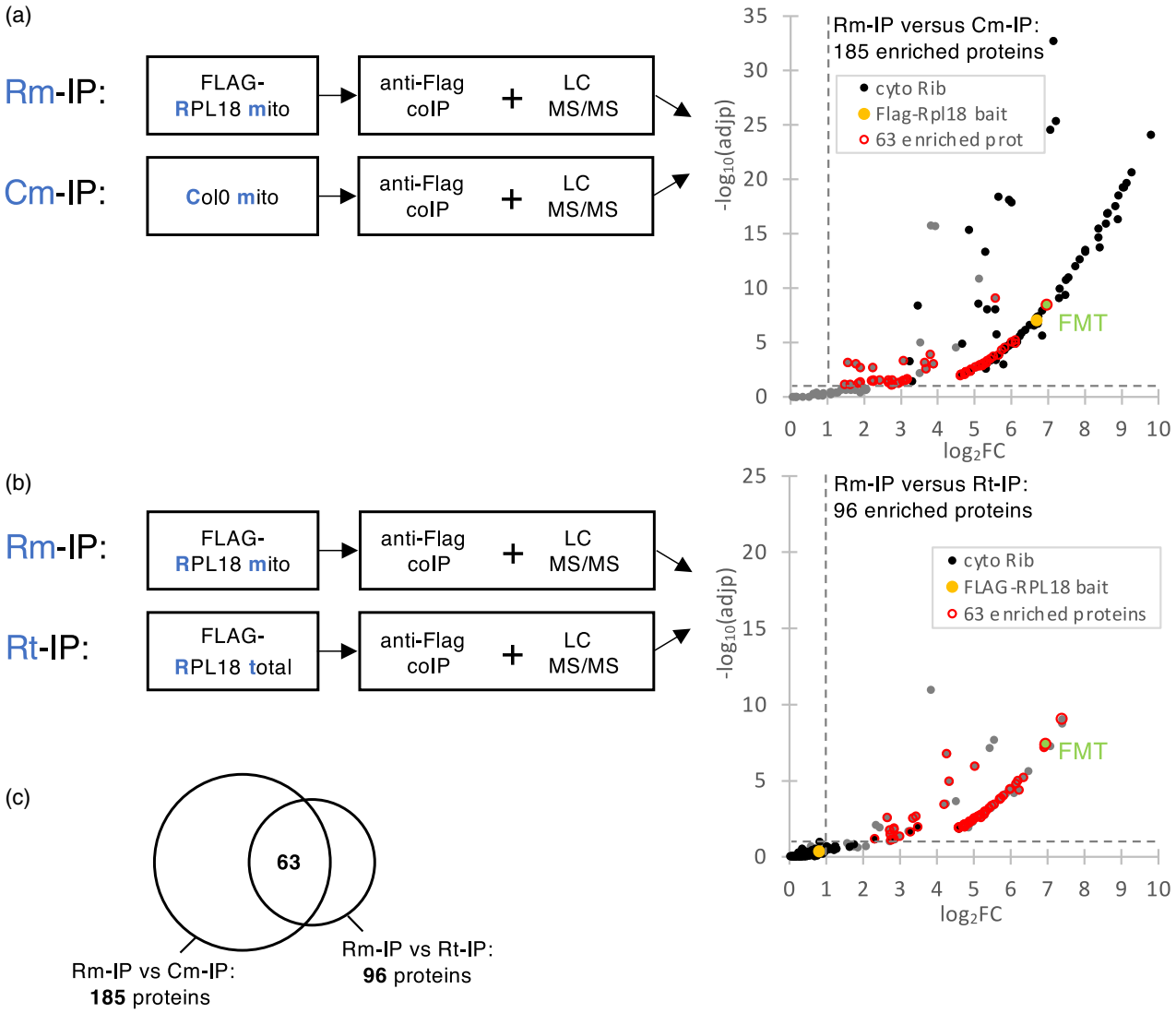

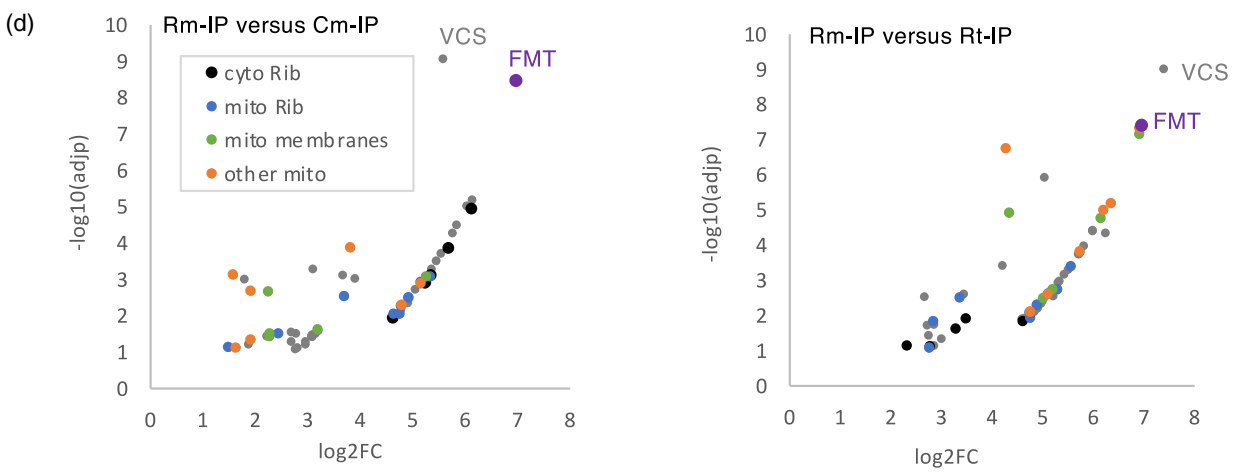

where interaction between cytosolic ribosomes and TOM complex has been found (Gold et al., 2017).

The most enriched proteins among the 63 are two cytosolic proteins: VCS (AT3G13300) and FMT (AT3G52140). VCS forms an mRNA decapping complex with DCP1 and DCP2 in processing bodies (P-bodies) (Xu & Chua, 2011). However, neither DCP1 (AT1G08370), nor DCP2 (AT5g13570) could be identified in any of the above IPs. FMT, a member of the CLUSTERED MITOCHONDRIA (CLU) family, is required for the correct distribution of mitochondria within the cell (El Zawily et al., 2014). Because of the properties of its orthologues and its role in plant mitochondria distribution (El Zawily et al., 2014), FMT was investigated further.

FMT is an RBP that strongly interacts with the ribosome at the surface of mitochondria

To explore the functions of FMT, it was essential to verify its localization in the cell. FMT has been previously shown to be only cytosolic, with a diffuse pattern but also as particles. Some of these particles were found to be associated and moving with mitochondria (Ayabe et al., 2021; El Zawily et al., 2014; Ma et al., 2021). We have constructed two translational fusions of FMT with GFP, one with GFP in N-terminal (GFP-FMT), the other with GFP in C-terminal (FMT-GFP), both under the control of the 35S promoter. *At* lines stably expressing the two FMT fusions were obtained. Both FMT fusions gave the expected cytosolic location, often with the punctuate distribution (Figure 2a, Figure S2a). When transiently expressed in *Nicotiana benthamiana*, the two FMT constructs also gave cytosolic signals, either diffuse, enriched around mitochondria or as foci. Many of these foci were associated and moved with mitochondria (Figure 2b, Figure S2b, Movies S1–S4).

To determine FMT interactants, mitochondrial proteins extracts were prepared from inflorescences of *At* lines expressing GFP-FMT or FMT-GFP and Col0. Proteins were immunoprecipitated with anti-GFP beads and identified by MS. The IPs were then compared, that is GFP-FMT with Col0 and FMT-GFP with Col0 (Figure 3a,b). Respectively, 73 and 28 proteins were found enriched in GFP-FMT and FMT-GFP compared to Col0, with cut-offs of FC above 2 and adj *p* below 0.1. In total, 75 proteins were co-purified with at least one of the two FMT constructs (Figure 3c,d; Table S2). Thirty-five of the 75 were cytosolic ribosomal proteins and 25 others were mitochondrial. CoIPs with anti-GFP beads were also performed with mitochondria from seedlings of the GFP-FMT line and Col0. Again, co-purification of FMT and cytosolic ribosomal proteins was obtained (Figure S3, Table S3). All these reverse coIPs confirmed that FMT co-purified with cytosolic ribosomes in mitochondrial fractions.

Because FMT is also cytosolic (Figure 2, Figure S2), coIPs were also performed with total extracts from inflorescences and seedlings of GFP-FMT and FMT-GFP lines, as well as of Col0. Only one ribosomal protein and one other protein (a mitochondrial pyruvate dehydrogenase complex subunit encoded by AT3G13930) were found enriched in FMT coIPs (Figure S4a,b). Seedlings total extracts were also crosslinked with formaldehyde before immunoprecipitation to withstand the isolation procedure. Under these conditions, 119 proteins were found enriched in FMT coIPs and 81 were ribosomal proteins (Figure S4c, Table S4).

Altogether, these coIPs revealed that FMT poorly or partially interacted with cytosolic ribosomes in a total extract. By contrast, FMT was found to strongly interact with cytosolic ribosomes in the mitochondrial fractions. Using coIP and yeast two-hybrid assays, Ayabe

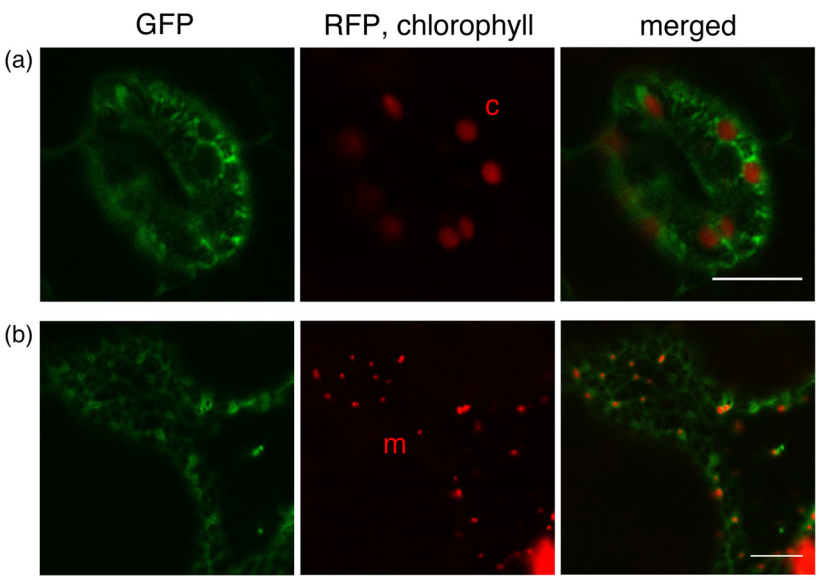

Figure 2. FMT localization in plant cells.
(a) *A. thaliana* 18-day-old seedlings stably expressing the GFP-FMT fusion (under the 35S promoter). The GFP signal showed diffuse cytosolic localization and also a punctuate distribution.
(b) *N. benthamiana* 6-week-old leaves transiently expressing the GFP-FMT and the mitochondrial pSU9-RFP.
Leaves were examined by confocal microscopy. GFP, GFP fluorescence; RFP, chlorophyll, chlorophyll autofluorescence in (a), mitochondrial pSU9-RFP fluorescence and chlorophyll autofluorescence in (b); merged, 'GFP' and 'RFP, chlorophyll' channels. c, chloroplast; m, mitochondrium. Scale bars = 10 μm.

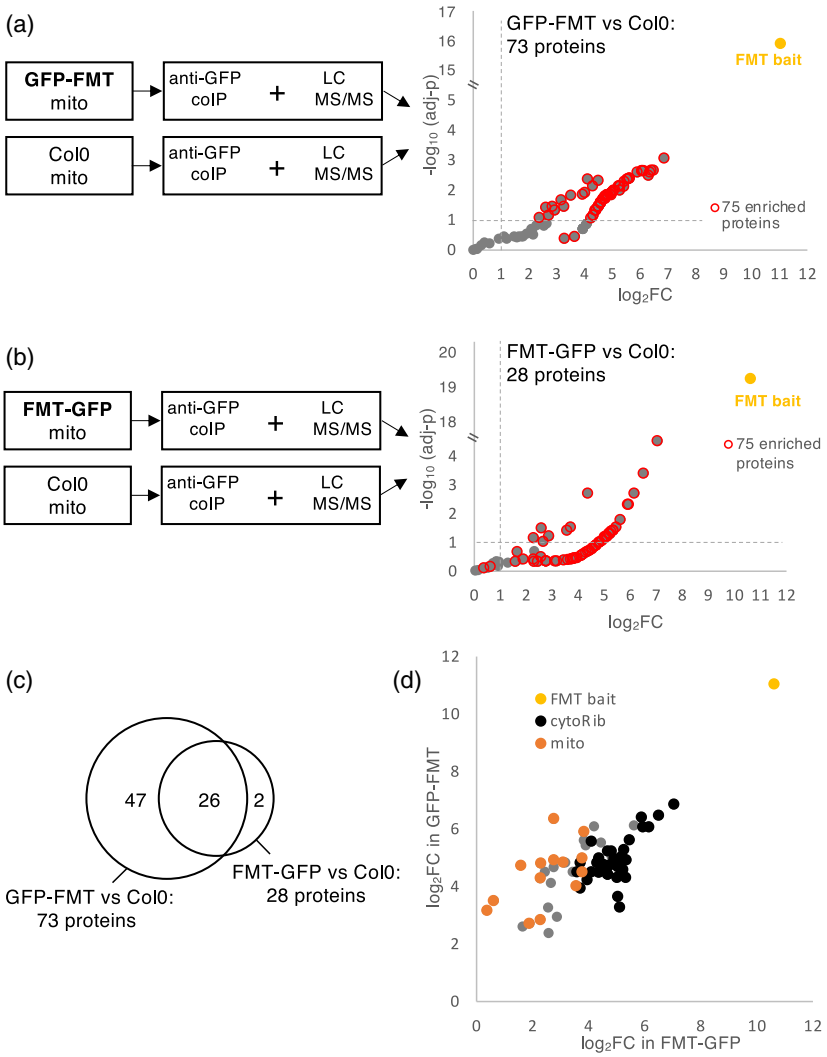

Figure 3. Identification of proteins co-purifying with FMT at the surface of inflorescence mitochondria.
(a) GFP-FMT mitochondrial coIP compared to Col0 mitochondrial coIP (GFP-FMT versus Col0).
Immunoprecipitated proteins were identified by LC–MS/MS. Statistical analyses based on specific spectral counts identified 73 proteins enriched in GFP-FMT compared to Col0 (cuts-off FC > 2 and adj $P < 0.1$).
(b) FMT-GFP mitochondrial coIP compared to Col0 mitochondrial coIP (FMT-GFP versus Col0).
With the same cuts-off as in (a), 28 proteins were enriched in FMT-GFP compared to Col0.
(c) In total, 75 proteins were enriched in at least one FMT/GFP IP. They are shown with a red circle in (a) and (b).
(d) The enrichment of the 75 proteins in FMT coIPs. The *x*- and *y*-axes correspond, respectively, to log_2FC in FMT-GFP and GFP-FMT coIPs. The FMT bait is shown in yellow. Proteins from cytosolic ribosomes are shown in black and mitochondrial proteins are shown in orange.

et al. (2021) have also shown the interaction of FMT with some proteins linked with translation.

The split-GFP approach (Romei & Boxer, 2019) was used to confirm the proximity of FMT with the ribosome and with the mitochondrial membrane. Translational fusions with either GFP-β11 strand or GFP-β1–10 strands were transitory co-expressed in *N. benthamiana* (Figure 4). The co-expression of β1–10-TOM5 and β11-FMT, on the one hand, and of β1–10-RPL18 and β11-FMT on the other hand, resulted in fluorescence, showing that these proteins pairs allow the complementation of the two GFP fragments in *N. benthamiana*. The split-GFP approach thus confirmed the proximity of FMT with the ribosome and with the mitochondrial surface.

To determine whether FMT was an RBP, an oligo(dT) capture experiment was performed. Leaves from wild-type Col0 were first irradiated with UV to induce covalent bonds between RNAs and interacting proteins. Then, the leaves extracts were used for the capture of poly(A) RNAs and their covalently linked proteins, using oligo(dT) magnetic beads. FMT was detected in the eluate, confirming its RNA binding property (Figure 5). The *Drosophila* and mammalian FMT orthologues have been also shown as RBPs (Gao et al., 2014; Sen & Cox, 2016).

Fmt KO is associated with reduced growth of seedlings and slightly affects the mitochondrial proteome

To identify FMT functions, an *fmt* KO mutant (SALK_056717) was analyzed. The T-DNA insertion in *the FMT* locus (AT3G52140) was verified (Figure S5a,b) and FMT protein was not detected in this line (Figure S5c). As already shown with other *fmt* mutants (El Zawily et al., 2014), *fmt* seedlings appeared to be smaller, with shorter primary roots, than wild-type (Figure S5d). The difference between *fmt* and Col0 was lost over time, and the delayed phenotype was no longer observed in older and flowering plants (Figure S5e). Finally, the clustering of mitochondria was observed in the SALK_056717 line (Figure S5f), as previously observed in

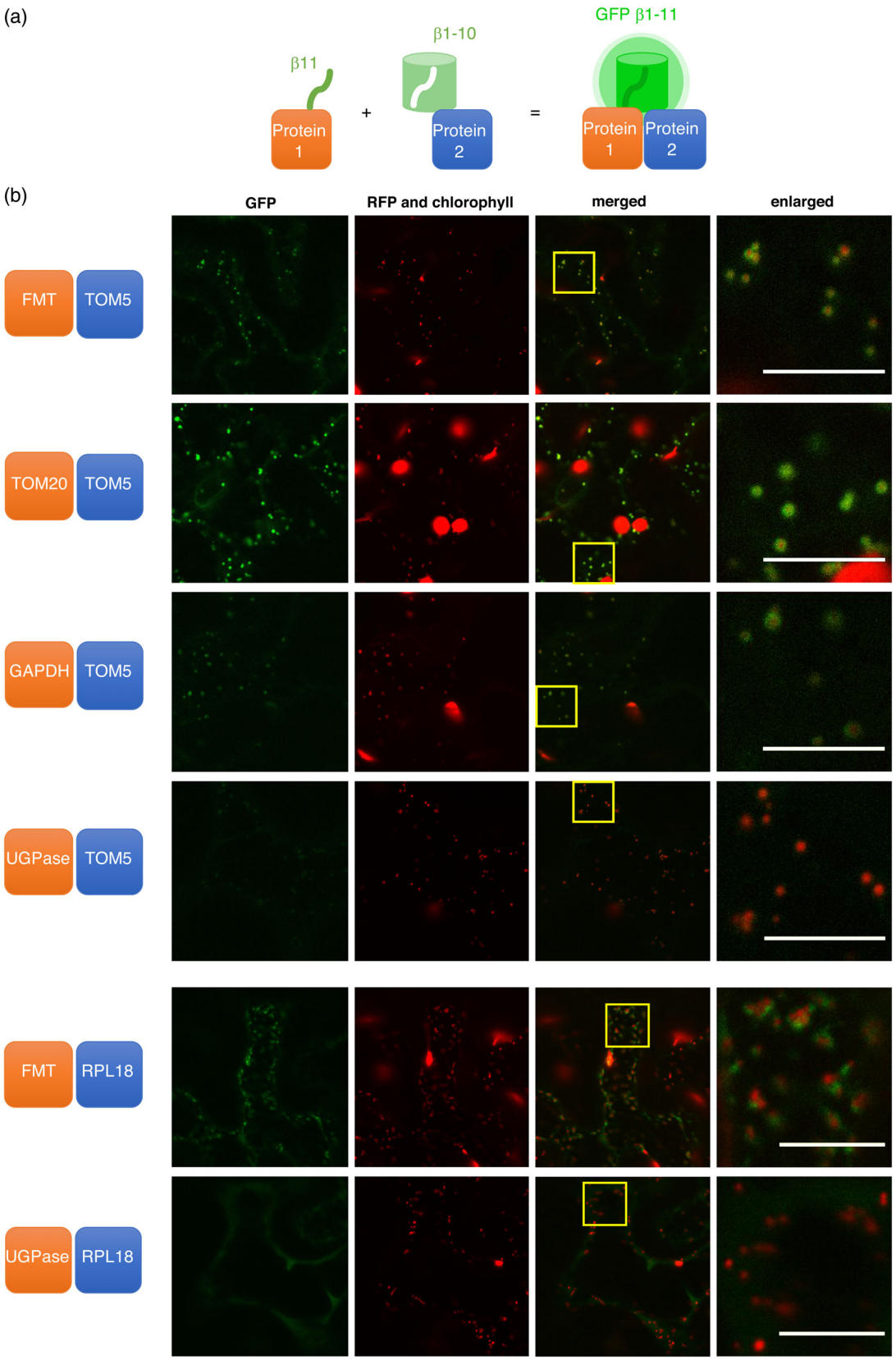

Figure 4. Split-GFP experiments.
(a) Schematic representation of the Split-GFP experiment. The proteins of interest were respectively fused with GFP-β11 strand (Protein 1, in orange) or GFP-β1–10 strands (Protein 2, in blue). *N. benthamiana* leaves were co-transformed with constructs encoding β1–10 and β11 fusions and with the mitochondrial pSU9-RFP construct. The co-localization of the two fusion proteins allowed the reconstitution of a functional GFP.
(b) Confocal imaging.
For interactions with mitochondria, the MOM TOM5 protein was fused with β1–10. The co-expression with FMT fused to β11 gave a signal around mitochondria. The TOM20–TOM5 and GAPDH-TOM5 pairs served as positive controls. TOM5 and TOM20 are two components of the TOM complex in MOM. The cytosolic GAPDH enzyme is found at the surface of mitochondria (Giege et al., 2003) and so the GAPDH-TOM5 pair is a positive control for the interaction of a cytosolic protein with MOM. By contrast, UGPase-TOM5 served as a negative control, with UGPase being only cytosolic.
For interactions with the ribosome, RPL18 was fused with β1–10. The co-expression with FMT fused to β11 gave a signal often associated with mitochondria. By contrast, the UGPase-RPL18 pair gave a very weak and diffuse signal in the cytosol.
GFP, GFP fluorescence; RFP and chlorophyll, mitochondrial pSU9-RFP fluorescence and chlorophyll autofluorescence. The yellow squares correspond to the enlarged images. Scale bars = 10 μm.

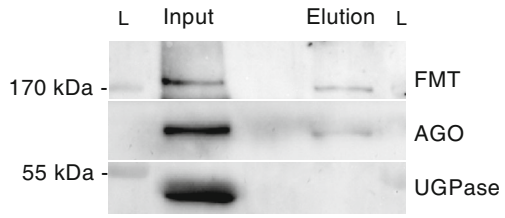

Figure 5. FMT is an RNA-binding protein.
Leaves from *At* Col0 (wild-type) were UV-irradiated to crosslink RNA and proteins. The crosslinked mRNA-protein complexes were pulled down by oligo-d$(T)_{25}$ beads. Input and elution fractions were then analyzed by Western blotting. FMT was detected in the elution fraction. ARGONAUTE 1 (AGO) and UGPAse, respectively, were used as positive and negative controls for oligo(dT) pull down. L, ladder.

EMS, SALK_046271 and SAIL_284_D06 *fmt* lines (Ayabe et al., 2021; El Zawily et al., 2014; Logan et al., 2003).

According to the *fmt* seedling phenotype (Figure S5d), seedling mitochondria were analyzed in more detail. The DNA, RNA and proteins contents were analyzed. The quantity of mitochondrial DNA in a total DNA extract appeared similar in Col0 and *fmt* (Figure 6a). Moreover, a global effect on mitochondrial-encoded RNAs was not observed in *the fmt* line (Figure 6b), even if some RNAs appeared to be weakly affected (COX1, RPS3, 18S). We also compared mitochondrial proteomes in seedlings of *fmt* and Col0. Mitochondrial extracts were analyzed by MS. Approximately 720 mitochondrial proteins were identified in each extract, and 72 proteins were enriched or depleted in *fmt* mitochondria compared to Col0 (Figure 6c; Table S5; Figure S6a). Eleven were over-expressed, including the three alternative oxidases, which was consistent with alternative oxidase (AOX) activity and Western blotting (see below, Figure 6d,e). Among the 61 down-regulated proteins, three were tricarboxylic acid cycle enzymes, six were components of the mitochondrial ribosome (Waltz et al., 2019) and 22 were from OXPHOS complexes, mostly from complex I (14 out of 22) (Senkler et al., 2017). The lower level of some mito-ribosomal proteins is consistent with the lower level of the mitochondrial 18S rRNA (Figure 6b).

A similar approach was performed with mitochondria from *fmt* and Col0 inflorescences. With the same criteria as for seedlings, only four proteins were found to be affected in *fmt* mitochondria (Figure S6b, Table S5), with all four also being affected in *fmt* seedling mitochondria. As already mentioned, the *fmt* flowering plants have no phenotype (Figure S5) and so it is not so surprising that the mitochondrial proteome of *fmt* inflorescences was only weakly affected.

Oxygen uptake was also measured in Col0 and *fmt* seedlings (Figure 6d), although no difference was observed between the two lines. The addition of cyanide (KCN), which blocks oxidative phosphorylation (OXPHOS pathway), and propyl gallate (PG), which blocks AOX, resulted in an increase of the AOX pathway but no apparent change in OXPHOS.

In summary, the reduced levels of some OXPHOS proteins were observed in seedling mitochondria, but they did not appear to affect significantly OXPHOS activity. For mitochondrial translation, some mito-ribosomal proteins were also found to be down-expressed in *fmt*. Proteome analysis showed that most of the 16 identified mitochondrial-encoded proteins appeared to be weakly depleted in *fmt* (Figure S6c), suggesting that the mitochondrial translation could be weakly affected in this mutant. Finally, increased levels of AOX proteins and AOX activity (Figure 6c–e) were observed in *fmt*. AOX have been usually considered as indicators of stress and mitochondrial dysfunction (Juszczuk et al., 2012; Robert et al., 2012; Saha et al., 2016).

The association of cytosolic mRNAs with the mitochondrial surface is disrupted in the *fmt* line

A microarray-based transcriptomic analysis has been previously performed in an EMS mutant of FMT (El Zawily et al., 2014) and only minor changes in mRNAs abundance were observed. Among the affected transcripts, some mRNAs coding for mitochondrial proteins have been identified as mitochondrial-associated in *Solanum tuberosum* (MLR RNAs) (Vincent et al., 2017). We have explored the expression and mitochondrial association of three such mRNAs: CIII-RISP (AT5G13430), coding for the RISP subunit in complex III (Li et al., 2019), and two complex I subunits, CI-51 (AT5G08530) and CI-7.5 (AT1G67785) (Klodmann & Braun, 2011).

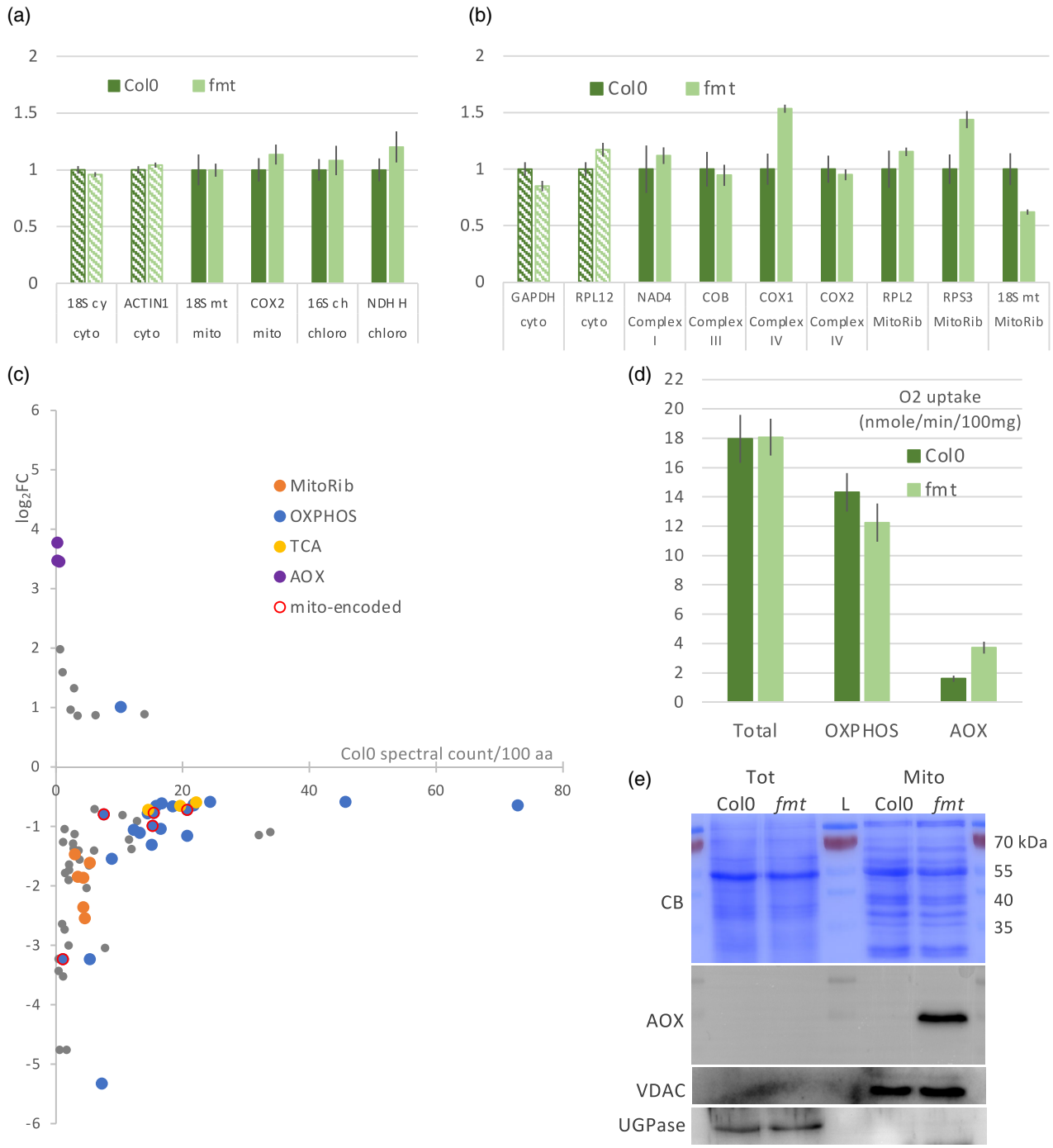

Figure 6. Analysis of mitochondria from *fmt* seedlings.
(a) Mitochondrial DNA content in total extracts. The level of organellar DNA was evaluated in total extracts of Col0 or *fmt* seedlings by qPCR. Normalization was performed with two nuclear genes coding for cytosolic 18S and actin, and the results are expressed relatively to Col0. The error bars correspond to SEM (biological repeats $n = 3$). (b) Mitochondrial RNA level in total extracts. The level of mitochondrial encoded RNAs was evaluated in total extracts of Col0 or *fmt* seedlings by RT-qPCR. Normalization was performed with two cytosolic transcripts (GAPDH and RPL12) and the results are expressed relatively to Col0. The error bars correspond to SEM (biological repeats $n = 3$). (c) Mitochondrial proteome. Proteins from purified mitochondria were analyzed by LC–MS/MS, and spectral count label-free quantifications were performed (*fmt* compared to Col0). With criteria [adj $P < 0.1$, FC > 1.5], 72 were found differently expressed in *fmt* mitochondria compared to Col0. The expression level in Col0 is presented on the *x*-axis (spectral count per 100 amino acids). The fold change is shown on the *y*-axis (*fmt* versus Col0). (d) O_2 uptake (nmol min^{-1} 100 mg^{-1} fresh seedlings): OXPHOS and AOX activities. Oxygen consumption was measured with an oxygraph. The addition of cyanide and of propygallate allowed to evaluate OXPHOS respiration and AOX activity (Figure S7) ($n = 10$). (e) Western blotting of total and mitochondrial extracts (15 μg) from 8-day-old *fmt* and Col0 seedlings. Immunodetection was performed with antibodies against the mitochondrial AOX, the mitochondrial VDAC and the cytosolic UGPase. CB, Coomassie Blue staining of the membrane.

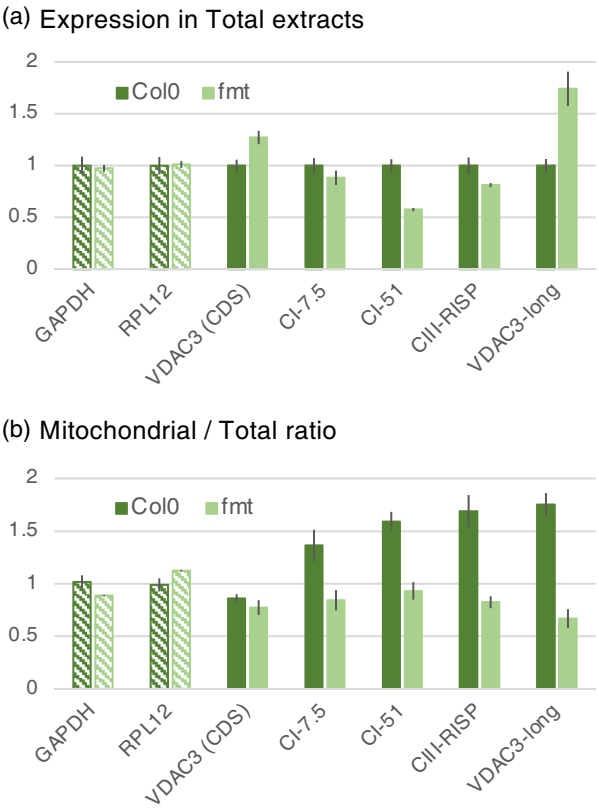

Figure 7. *fmt* mutation disturbs mRNA targeting to the mitochondrial surface.

Messenger RNAs were quantified by RT-qPCR in mitochondrial and total extracts from seedlings. To compare the three biological replicates, normalization was performed with GAPDH and RPL12 mRNAs. (a) Total extracts: the quantity of each mRNA in *fmt* total extracts was expressed relative to its level in wild-type Col0. (b) Mitochondrial/total ratio. The quantity of each mRNA in the mitochondrial fraction was corrected by its quantity in the total fraction to take into account the expression level of the gene. Mitochondrial/total ratios were expressed relative to the mean of GAPDH and RPL12 ratios. Error bars represent the SEM ($n = 3$).

GAPDH, glyceraldehyde 3-phosphate dehydrogenase (AT1G13440); RPL12, cytosolic ribosomal protein L12A (AT2G37190); VDAC3, mitochondrial voltage-dependent anion channel 3 (AT5G15090) [VDAC3 (CDS) corresponds to both VDAC3 mRNAs isoforms, VDA3-long only corresponds to the long mRNA isoform]; CIII-RISP, RISP subunit in complex III (AT5G13430); CI-51 (AT5G08530) and CI-7.5 (AT1G67785), 51- and 7.5-kDa proteins in complex I.

In addition, in *A. thaliana*, a well-studied targeted mRNA is VDAC3 (AT5G15090). The VDAC3 gene has previously been shown to be transcribed into two isoforms that differ by the length of their 3′ UTR. The long isoform was found at the surface of mitochondria, but not the short one (Michaud et al., 2014).

To test the impact of *fmt* mutation on these mRNAs, total and mitochondrial RNAs were extracted from Col0 and *fmt* seedlings and a quantitative RT-PCR (RT-qPCR) was performed. CI-51 appeared to be down expressed in *fmt* total extracts, but not CI-7.5 or CIII-RISP. By contrast, VDAC3-long appeared overexpressed in *fmt*, which is consistent with the fact that this isoform is highly sensitive to stress (Hemono et al., 2020) (Figure 7a).

As reported previously (Michaud et al., 2014), VDAC short and long isoforms differ in their association with mitochondria. The three other mRNAs were found enriched in the Col0 mitochondrial fraction compared to the VDAC3 short isoform. However, in the *fmt* line, the mitochondrial associations of the four mRNAs appeared similar to the non-targeted VDAC3 short isoform mRNA (Figure 7b), suggesting a role of FMT protein in the mRNA association with the mitochondrial surface.

CIII-RISP and CI-51 proteins were identified in the mitochondrial proteome, and both were among the 61 down-regulated proteins in *fmt* (Figure 6c). The steady-state of CIII-RISP protein decreased, whereas the steady-state of its mRNA was not clearly affected, suggesting a correlation between mRNA localization and protein abundance in mitochondria. The decrease in CI-51 protein could be explained by the decrease in its mRNA level and/or in its mRNA association with mitochondria. For CI-7.5 and VDAC3 proteins, no hypothesis could be made because CI-7.5 was not detected in the proteome, and two mRNAs with different behaviors code for the same VDAC3 protein.

DISCUSSION

FMT is an evolutionarily conserved protein belonging to the CLU family, and is found in species as distant as plants, yeast, amoeba, flies or mammals. FMT contains numerous domains, which are conserved in the other proteins of the CLU family (Figure S8). The exact function of each of these domains has not been clearly established, even if all were shown to be essential for normal development and mitochondrial functions in *Drosophila* (Sen & Cox, 2016). The most studied domain is a tetratricopeptide repeat (TPR) domain in the distal part of the proteins. This TPR domain has been shown to facilitate mRNA binding in *Drosophila* (Sen & Cox, 2016) and human cells (Hemono et al., 2022). It is also involved in CLUH self-interaction and for interaction with other proteins (Hemono et al., 2022). For FMT, yeast two-hybrids assays have shown that the different domains are involved in protein–protein interactions (Ayabe et al., 2021).

We have shown here that FMT interacts with both RNAs and proteins. FMT is a cytosolic protein, presenting either a diffuse localization or organized in foci, and is often found near the mitochondria. By coIP and reverse coIP experiments, we have found that FMT copurifies with cytosolic ribosome, but only in mitochondrial fractions. We have confirmed the proximity of FMT with cytosolic ribosomes and with mitochondria by split-GFP experiments.

As for all proteins of the CLU family, the *fmt* KO mutation induces the clustering of mitochondria. The *fmt* mutation was also found to have a decreased capacity to fight bacterial infection (Vellosillo et al., 2013). The

consequences of the mutation on plants grown in standard conditions were evident at the level of seedlings, with growth retardation, although this phenotype faded during development. At the mitochondria level, the mitochondrial proteome from seedlings appeared to be affected, with a decrease in the abundance of OXPHOS proteins and components of the mitoribosome. On the other hand, AOX proteins were overexpressed, suggesting mitochondrial stress. The dysfunction of the mitochondria in young plants is confirmed by the high proportion of depolarized mitochondria in *fmt* mutant (Ma et al., 2021; Nakamura et al., 2020). However, the defect in the mitochondrial proteome was no longer visible in inflorescences, which is consistent with the absence of phenotype in flowering plants. Accordingly, the function of FMT appears to be particularly important in the early stages of development.

Mitochondrial biogenesis relies on the massive import of proteins encoded by the nuclear genome. This import can occur post-translationally or co-translationally. In this last case, the mRNAs are sent to the surface of the mitochondria, where cytosolic ribosomes translate them, and the proteins are directly imported into the mitochondria. Finding FMT associated with cytosolic ribosomes in mitochondrial fractions prompted us to explore the co-translational import pathway. This pathway still remains little studied in *A. thaliana*, and only a single mRNA, VDAC3-long, has been identified so far on the surface of mitochondria (Michaud et al., 2014). Therefore, we looked for other potential candidates among the mRNAs for which expression is reduced in *fmt* mutants (El Zawily et al., 2014). We have thus selected three mRNAs for which the orthologs in *S. tuberosum* are targeted to the mitochondrial surface (Vincent et al., 2017). These three mRNAs and VDAC3-long were no longer enriched at the mitochondrial surface in *fmt* mutant, showing the implication of FMT in the targeting and/or anchoring of these mRNAs to the mitochondrial surface.

The localization of an mRNA on the mitochondrial surface requires its transport from the nucleus to the mitochondria and its docking to the mitochondria, where it would be translated. These mechanisms are still poorly understood, with the intervention of multiple signals (on the mRNA and/or on the protein) and various protein factors. FMT is an abundant RBP in the cytosol. It is also found to be associated with ribosomes on the mitochondrial surface. FMT could therefore be involved, directly or indirectly, in the targeting of its target mRNAs, their anchoring on mitochondria or their localized translation.

Proteins of the CLU family have been shown to affect the translation of some mRNAs coding for mitochondrial proteins (Gao et al., 2014; Schatton et al., 2017). Moreover, different teams have also demonstrated a link between CLU proteins and translation at the surface of mitochondria (Hemono et al., 2022; Sen & Cox, 2016; Vardi-Oknin & Arava, 2019). Thus, in *Drosophila*, Sen and Cox (2016) have demonstrated the association of Clueless with the ribosomes on MOM, and suggest that the role of Clueless is to facilitate mRNA association with the ribosome at the mitochondrial surface. On the other hand, Hemono et al. (2022) demonstrated an enrichment of certain mRNAs in the mitochondrial fraction of CLUH KO human cells, while other mRNAs are not affected. In addition, Vardi-Oknin and Arava (2019) have shown that CLUH depletion in human cells causes a decrease in the amount of ribosomes associated with mitochondria, whereas there is an increase in the association of particular mRNAs with the remaining mitochondria proximal ribosomes. In plants, we have shown that *fmt* KO mutation induces a decrease in the amount of at least some RNAs associated with mitochondria. These apparent discrepancy between studies and/or organisms need to be further explored, for example, through genome wide analysis and taking into account biological material and growth conditions. The unifying message is that proteins from the CLU family appear to be involved in the localization of some mRNAs coding for mitochondrial proteins and their localized translation.

The role of FMT in mRNA localization and translation should be also explored further as part of the latest discoveries on FMT, which has recently been shown to be associated with mitophagy processes. Ma et al. (2021) have shown that treatment with a decoupling agent induces mitophagy and a reorganization of FMT in foci, some of which co-localize with mitochondria. In addition, FMT has been shown to associate with ATG8, a mitophagosome marker. Nakamura et al. (2020) have shown that the clustering of the mitochondria was higher in an *atg5/fmt* double mutant than in a *fmt* mutant (ATG5 is also involved in mitophagy). El Zawily et al. (2014) have proposed that FMT regulates inter-mitochondrial association, which is a necessary step in mitochondrial fusion. Moreover, mitophagy is closely linked with the mitochondrial fusion/fission balance. Finally, in the present study, we have demonstrated that FMT is associated with ribosomes at the surface of mitochondria. We could suggest that FMT would control the localization and/or translation of mRNAs coding for proteins involved in the fusion/fission/mitophagy processes. Therefore, the relationship between FMT and mitophagy needs to be explored further.

Finally, a last point to be addressed concerns the link between FMT and chloroplasts. Photosystem I activity is reduced in *fmt* (El Zawily et al., 2014). Moreover, the de-etiolation of seedlings germinated under dark conditions is reduced in *fmt* and also in *atg5* (Ma et al., 2021). These results suggest that the role of FMT might not be limited to mitochondria but could also impact inter-organellar communications and, consequently, the functioning of the plant cell in response to development and/or biotic or abiotic signals.

EXPERIMENTAL PROCEDURES

Plant material and growth conditions

Arabidopsis plants were grown in long-day conditions (16:8 h light/dark photocycle at 21°C and 18°C cycles; LED tubes Philips 1500 mm SO 20 W 840 T8; Philips, Eindhoven, The Netherlands; photon flux density of 120 μmol sec^{-1} m^{-2} at the plant level). Seedlings were grown for 8 days in hydroponic cultures at 23°C with constant light in Murashige and Skoog MS231 medium (Duchefa, Haarlem, The Netherlands).

The *fmt* insertion mutant SALK_056717 was from Columbia ecotype. The line expressing the epitope-tagged ribosomal protein, FLAG-RPL18 (AT3G05590), was from (Zanetti et al., 2005). FMT-GFP, GFP-FMT and MS2-GFP lines were obtained by floral dip with pAM557, pAM549 and pAM495 plasmids respectively (Table S6) (Clough & Bent, 1998).

Transient transformation of *At* and *N. benthamiana* was performed by infiltration of leaves with a suspension of *Agrobacterium tumefaciens* harboring different constructs. The constructs allowed the expression of different GFP or split-GFP fusion proteins, the pSU9-RFP mitochondrial marker (Michaud et al., 2014), the COXIV-GFP mitochondrial marker (Peeters et al., 2000) and the silencing suppressor P19 protein (Michaud et al., 2014).

Genotyping

Genomic DNA was extracted from rosette leaves of 4-week-old *At* plants as described previously (Edwards et al., 1991) and subjected to a PCR-based screening using primer pairs 1–2 and 1–3 (1: 5′-CAACCCATCACCAAGAAGGGTC-3′; 2: 5′-CATGGTACAAAACCATAGCCAGG-3′; 3: 5′-TGGTTCACGTAGTGGGCCATCG-3′). PCR products were separated by agarose gel electrophoresis and visualized by ethidium bromide staining.

qPCR

According to the manufacter's instructions, genomic DNA for qPCR was extracted from 8-day-old water-cultured seedlings using a NucleoSpin® plant L kit (Macherey-Nagel, Düren, Germany). For qPCR, three biological replicates were performed. DNA was used at 3 ng μl^{-1} and diluted10 times, and three technical replicates were performed for each dilution. The qPCR efficiency for each primers couple was determined by dilutions of DNA. The qPCR results were normalized with the nuclear genes coding for actin (ACTIN1) and 18S ribosomal RNA (18S cy) (Table S7) to compare the different replicates.

RNA extraction, reverse transcription and RT-qPCR

RNA was extracted from mitochondria and whole cells using Tri Reagent® (Molecular Research Center, Cincinnati, OH, USA) in accordance with the manufacter's instructions, then treated with RNase free-DNase RQ1 (Promega, Madison, WI, USA) and quantified with a Nanodrop spectrophotometer (Thermo Scientific, Waltham, MA, USA). Their quality was checked by electrophoresis in MOPS buffer/formaldehyde/agarose gel. Reverse transcription was performed with Reverse Transcription SuperScript™ IV (Invitrogen, Waltham, MA, USA) in presence of hexamers and oligo(dT) primer (Michaud et al., 2010). For qPCR, the RT was used directly and diluted10 times, and two or three technical replicates were performed for each dilution. Three biological replicates, corresponding to mitochondrial and total RNA extracted from the same plant material, were prepared. The qPCR efficiency for each primers pair was determined by dilutions of cDNA. To compare the different replicates, the qPCR results were normalized with the cytosolic ribosomal protein L12 (RPL12, AT2G37190) and glyceraldehyde 3-phosphate dehydrogenase (GAPDH, AT1G13440) mRNAs.

Mitochondria preparation

Gradient-purified mitochondria were prepared from 8-day-old water-cultured seedlings as described previously (Hemono et al., 2020) or from inflorescences of 6/8-week-old *Arabidopsis thaliana* as described previously (Waltz et al., 2019).

Immunoprecipitation

Proteins were extracted from grounded seedlings or inflorescences or from corresponding mitochondria. μMACS™ GFP or μMACS™ DYKDDDDK (FLAG) Protein Isolation Kits (Miltenyi Biotec, Bergisch Gladbach, Germany) were used for immunoprecipitations. Three biological repeats were performed. For seedling material, the composition of the lysis buffer was [50 mM Tris-HCl, pH 8, 50 mM NaCl, 10 mM $MgCl_2$, 1% Triton X-100, 200 μg ml^{-1} cycloheximide, protease inhibitors (cOmplete™, EDTA-free protease inhibitor cocktail, 1 tabletper 50 ml; Roche, Basel, Switzerland)]. The wash buffer corresponded to the lysis buffer but with 0.1% Triton X-100. For inflorescence material, the composition of the lysis buffer was (20 mM HEPES-KOH, pH 7.6, 100 mM KCl, 20 mM $MgCl_2$, 1 mM DTT, 1% Triton X-100, 20 μg ml^{-1} cycloheximide, protease inhibitors). The wash buffer corresponded to the lysis buffer but with 0.1% Triton X-100.

Proteomic analyses

RPL18 and FMT immunoprecipitated samples were prepared for MS analyses as described previously (Hemono et al., 2022). For mitochondrial protein extracts, after a Bradford colorimetric assay (Bio-Rad, Hercules, CA, USA), 10 μg of sample was prepared using the same protocol. Data were searched against the TAIR10 *A. thaliana* database. All these steps were performed at the "Plateforme Protéomique Strasbourg-Esplanade" (http://www-ibmc.u-strasbg.fr/proteo/Web/accueil.htm) (Method S1).

To identify significantly affected proteins, a statistical analysis based on spectral counts was performed using a R package (https://github.com/hzuber67/lPinquiry4) as described previously (Scheer et al., 2021). To avoid too much bias, only proteins with a mean of at least three spectra in the most expressed condition were further considered. Mitochondrial localization was determined according to SUBA4 (http://suba.live) (Hooper et al., 2017).

Western blotting and antibodies

Western blotting analysis was conducted according to standard. Antibodies against AOX (T. Elthon, GT monoclonal antibodies, University of Nebraska, Lincoln, NE, USA) (Elthon et al., 1989), UGPase, AGO and Arf1 (https://www.agrisera.com; AS05 086, AS09 527 and AS08325, respectively), GFP and VDAC (A. Dietrich, IBMP, Strasbourg, France), and calnexin (C. Ritzenthaler, IBMP, Strasbourg, France) were used. For the FMT antibody, the peptide corresponding to the C-terminal part of FMT (373 aminoacids) was purified via SDS-PAGE and injected into rabbits (Covalab antibody production).

Confocal microscopy

N. bentamiana leaves were observed 2 days after agroinfiltration. *A. thaliana* or *N. bentamiana* leaves were directly observed by using a LSM780 confocal microscope (Zeiss, Oberkochen, Germany). GFP and RFP fluorophores were excited at 488 and

561 nm, respectively, and emission signals were simultaneously collected at 490–535 nm for GFP and at 555–700 nm for RFP.

Oligo(dT) affinity purification of crosslinked protein–RNA complexes

Oligo(dT) capture was performed as described previously (Bach-Pages et al., 2020) with minor modifications. For crosslinking, leaves of *At* Col0 were placed on ice and irradiated in a Stratalinker (Stratagene, Santa Clara, CA, USA) with 254-nm UV light at 1000 mJ cm^{-2}. The irradiation was performed twice with a 1-min pause in between treatments. After irradiation, leaves were immediately frozen in liquid N_2 and ground into fine powder. The powder (1.1 g) was resuspended in 11 ml of lysis buffer [20 mM Tris HCl, pH 7.5, 500 mM LiCl, 0.5% LiDS, 1 mM EDTA, 0.2% IGEPAL, 2.5% PVP40 (wt/v), 1% B-ME (v/v), 5 mM DTT, protease inhibitor and Vanadyl RNase inhibitor] and incubated for 10 min on a rotator at 4°C. The lysate was cleared by two centrifugations (3200 ***g*** for 10 min at 4°C and 20 000 ***g*** for 10 min at 4°C) and filtered (Miracloth, 475 855-1R; Merck, Darmstadt, Germany). The lysate (input) was then incubated with 200 µl of oligo (dT)25 magnetic beads (New England Biolabs, Ipswich, MA, USA) for 1 h at 4°C on a rotator. Beads were collected on a magnet, washed twice with 1 ml of lysis buffer, twice with 1 ml of buffer I (20 mM Tris HCl, pH 7.5, 500 mM LiCl, 0.1% LiDS, 1 mM EDTA and 5 mM DTT), twice with 1 ml of buffer II (20 mM Tris HCl, pH 7.5, 500 mM LiCl, 1 mM EDTA and 5 mM DTT) and twice with 1 ml of buffer III (20 mM Tris HCl, pH 7.5, 200 mM LiCl, 1 mM EDTA, and 5 mM DTT). Beads were resuspended in 100 µl of protein extraction buffer (8 M urea, 50 mM Tris HCL, pH 6.9, 1 mM EDTA, 5% β-mercaptoethanol) and used for immunoblotting.

O_2 consumption

Oxygen consumption of seedlings was measured in 2 ml of culture medium with a liquid-phase Oxytherm oxygen electrode system (Hansatech Instruments, Pentney, UK). Five-day-old seedlings grown in liquid phase (30–40 mg) were directly imbibed in the electrode chamber and oxygen consumption rates were measured. After 6 min, KCN was added (final concentration of 2.5 mM), and oxygen consumption was re-measured. Differences between these two rates corresponded to cyanide-sensitive oxygen uptake (OXPHOS oxygen uptake). Then, after 8 min, PG was added (final concentration of 2.5 mM) and oxygen consumption was re-measured. Differences between the KCN and the PG rates correspond to AOX oxygen uptake.

ACKNOWLEDGEMENTS

This work was supported by the Université de Strasbourg and Centre National de la Recherche Scientifique (CNRS), by the French Agence Nationale de la Recherche (ANR-18-CE12-0021-01 'Polyglot') and by the French National Program 'Investissement d'Avenir' (ANR-11-LABX-0057 'MitoCross' LabEx). MH has a fellowship from MitoCross and JR has a fellowship from Polyglot. This work of the Interdisciplinary Thematic Institute IMCBio, conducted as part of the ITI 2021–2028 program of the University of Strasbourg, CNRS and Inserm, was supported by IdEx Unistra (ANR-10-IDEX-0002), STRAT'US (ANR 20-SFRI-0012) and EUR IMCBio (ANR-17-EURE-0023) under the framework of the French Investments for the Future Program.

AUTHOR CONTRIBUTIONS

MH, TSG, JR, AV, PH and EU were responsible for the experiments. PN and AMD were responsible for writing and editing.

CONFLICT OF INTEREST

The authors declare no conflict of interest.

SUPPORTING INFORMATION

Additional Supporting Information may be found in the online version of this article.

Figure S1. Quality control of proteins extracts.

Figure S3. Identification of proteins co-purifying with FMT at the surface of seedling mitochondria.

Figure S4. Identification of proteins co-purifying with FMT in total extracts from inflorescences, seedlings and seedlings after formaldehyde crosslinking.

Figure S5. Characterization of *fmt* KO line SALK_056717.

Figure S6. Mitochondrial proteomes in seedlings and inflorescences.

Figure S7. O_2 consumption in seedlings.

Figure S8. FMT organization and comparison with other CLU proteins.

Figure S2. FMT localization in plant cells, using the FMT-GFP fusion.

Method S1. LC–MS/MS protocol.

Movie S1. FMT localization and dynamic in plant cells.

Movie S2. FMT localization and dynamic in plant cells.

Movie S3. FMT localization and dynamic in plant cells.

Movie S4. FMT localization and dynamic in plant cells.

Table S1. Enriched proteins in co-immunoprecipitations from FLAG-RPL18 mitochondria.

Table S2. Enriched proteins in FMT co-immunoprecipitations from inflorescences mitochondrial extracts.

Table S3. Enriched proteins in FMT co-immunoprecipitation from seedling mitochondrial extracts.

Table S4. Enriched proteins in FMT co-immunoprecipitation from seedling total extracts after formaldehyde crosslinking.

Table S5. Comparison of mitochondrial proteome in *fmt* and Col0 seedlings.

Table S6. DNA constructs and plasmids.

Table S7. oligonucleotides used in qPCR and RT-qPCR.

REFERENCES

Ayabe, H., Kawai, N., Shibamura, M., Fukao, Y., Fujimoto, M., Tsutsumi, N. et al. (2021) FMT, a protein that affects mitochondrial distribution, interacts with translation-related proteins in Arabidopsis thaliana. *Plant Cell Reports*, **40**, 327–337.

Bach-Pages, M., Homma, F., Kourelis, J., Kaschani, F., Mohammed, S., Kaiser, M. et al. (2020) Discovering the RNA-binding proteome of plant leaves with an improved RNA interactome capture method. *Biomolecules*, **10**, 661.

Clough, S.J. & Bent, A.F. (1998) Floral dip: a simplified method for agrobacterium-mediated transformation of Arabidopsis thaliana. *The Plant Journal*, **16**, 735–743.

Edwards, K., Johnstone, C. & Thompson, C. (1991) A simple and rapid method for the preparation of plant genomic DNA for PCR analysis. *Nucleic Acids Research*, **19**, 1349.

El Zawily, A.M., Schwarzlander, M., Finkemeier, I., Johnston, I.G., Benamar, A., Cao, Y. et al. (2014) FRIENDLY regulates mitochondrial distribution, fusion, and quality control in Arabidopsis. *Plant Physiology*, **166**, 808–828.

Elthon, T.E., Nickels, R.L. & McIntosh, L. (1989) Monoclonal antibodies to the alternative oxidase of higher plant mitochondria. *Plant Physiology*, **89**, 1311–1317.

Fazal, F.M., Han, S., Parker, K.R., Kaewsapsak, P., Xu, J., Boettiger, A.N. et al. (2019) Atlas of subcellular RNA localization revealed by APEX-seq. *Cell*, **178**, 473–490.e26.

Funfschilling, U. & Rospert, S. (1999) Nascent polypeptide-associated complex stimulates protein import into yeast mitochondria. *Molecular Biology of the Cell*, **10**, 3289–3299.

Gao, J., Schatton, D., Martinelli, P., Hansen, H., Pla-Martin, D., Barth, E. et al. (2014) CLUH regulates mitochondrial biogenesis by binding mRNAs of nuclear-encoded mitochondrial proteins. *The Journal of Cell Biology*, **207**, 213–223.

Giege, P., Heazlewood, J.L., Roessner-Tunali, U., Millar, A.H., Fernie, A.R., Leaver, C.J. et al. (2003) Enzymes of glycolysis are functionally associated with the mitochondrion in Arabidopsis cells. *Plant Cell*, **15**, 2140–2151.

Gold, V.A., Chroscicki, P., Bragoszewski, P. & Chacinska, A. (2017) Visualization of cytosolic ribosomes on the surface of mitochondria by electron cryo-tomography. *EMBO Reports*, **18**, 1786–1800.

Hemono, M., Haller, A., Chicher, J., Duchêne, A.M. & Ngondo, R.P. (2022) The interactome of CLUH reveals its association to SPAG5 and its co-translational proximity to mitochondrial proteins. *BMC Biology*, **20**, 13.

Hemono, M., Ubrig, E., Azeredo, K., Salinas-Giege, T., Drouard, L. & Duchene, A.M. (2020) Arabidopsis voltage-dependent anion channels (VDACs): overlapping and specific functions in mitochondria. *Cell*, **9**, 1023.

Hooper, C.M., Castleden, I.R., Tanz, S.K., Aryamanesh, N. & Millar, A.H. (2017) SUBA4: the interactive data analysis Centre for Arabidopsis subcellular protein locations. *Nucleic Acids Research*, **45**, D1064–D1074.

Juszczuk, I.M., Szal, B. & Rychter, A.M. (2012) Oxidation-reduction and reactive oxygen species homeostasis in mutant plants with respiratory chain complex I dysfunction. *Plant, Cell & Environment*, **35**, 296–307.

Kellems, R.E., Allison, V.F. & Butow, R.A. (1974) Cytoplasmic type 80 S ribosomes associated with yeast mitochondria. II. Evidence for the association of cytoplasmic ribosomes with the outer mitochondrial membrane in situ. *The Journal of Biological Chemistry*, **249**, 3297–3303.

Klodmann, J. & Braun, H.P. (2011) Proteomic approach to characterize mitochondrial complex I from plants. *Phytochemistry*, **72**, 1071–1080.

Lashkevich, K.A. & Dmitriev, S.E. (2021) mRNA targeting, transport and local translation in eukaryotic cells: from the classical view to a diversity of new concepts. *Molecular Biology*, **55**, 507–537.

Lesnik, C., Cohen, Y., Atir-Lande, A., Schuldiner, M. & Arava, Y. (2014) OM14 is a mitochondrial receptor for cytosolic ribosomes that supports co-translational import into mitochondria. *Nature Communications*, **5**, 5711.

Lesnik, C., Golani-Armon, A. & Arava, Y. (2015) Localized translation near the mitochondrial outer membrane: an update. *RNA Biology*, **12**, 801–809.

Li, L., Lavell, A., Meng, X., Berkowitz, O., Selinski, J., van de Meene, A. et al. (2019) Arabidopsis DGD1 SUPPRESSOR1 is a subunit of the mitochondrial contact site and cristae organizing system and affects mitochondrial biogenesis. *Plant Cell*, **31**, 1856–1878.

Logan, D.C., Scott, I. & Tobin, A.K. (2003) The genetic control of plant mitochondrial morphology and dynamics. *The Plant Journal*, **36**, 500–509.

Ma, J., Liang, Z., Zhao, J., Wang, P., Ma, W., Mai, K.K. et al. (2021) Friendly mediates membrane depolarization-induced mitophagy in Arabidopsis. *Current Biology*, **31**, 1931–1944.e1934.

Michaud, M., Marechal-Drouard, L. & Duchene, A.M. (2010) RNA trafficking in plant cells: targeting of cytosolic mRNAs to the mitochondrial surface. *Plant Molecular Biology*, **73**, 697–704.

Michaud, M., Ubrig, E., Filleur, S., Erhardt, M., Ephritikhine, G., Marechal-Drouard, L. et al. (2014) Differential targeting of VDAC3 mRNA isoforms influences mitochondria morphology. *Proceedings of the National Academy of Sciences of the United States of America*, **111**, 8991–8996.

Nakamura, S., Hagihara, S., Otomo, K., Ishida, H., Hidema, J., Nemoto, T. et al. (2020) Autophagy contributes to quality control of leaf mitochondria. *Plant & Cell Physiology*, **62**, 229–247.

Peeters, N.M., Chapron, A., Giritch, A., Grandjean, O., Lancelin, D., Lhomme, T. et al. (2000) Duplication and quadruplication of Arabidopsis thaliana cysteinyl- and asparaginyl-tRNA synthetase genes of organellar origin. *Journal of Molecular Evolution*, **50**, 413–423.

Robert, N., d'Erfurth, I., Marmagne, A., Erhardt, M., Allot, M., Boivin, K. et al. (2012) Voltage-dependent-anion-channels (VDACs) in Arabidopsis have a dual localization in the cell but show a distinct role in mitochondria. *Plant Molecular Biology*, **78**, 431–446.

Romei, M.G. & Boxer, S.G. (2019) Split green fluorescent proteins: scope, limitations, and outlook. *Annual Review of Biophysics*, **48**, 19–44.

Saha, B., Borovskii, G. & Panda, S.K. (2016) Alternative oxidase and plant stress tolerance. *Plant Signaling & Behavior*, **11**, e1256530.

Saint-Georges, Y., Garcia, M., Delaveau, T., Jourdren, L., Le Crom, S., Lemoine, S. et al. (2008) Yeast mitochondrial biogenesis: a role for the PUF RNA-binding protein Puf3p in mRNA localization. *PLoS One*, **3**, e2293.

Salih, K.J., Duncan, O., Li, L., Trosch, J. & Millar, A.H. (2020) The composition and turnover of the Arabidopsis thaliana 80S cytosolic ribosome. *The Biochemical Journal*, **477**, 3019–3032.

Schatton, D., Pla-Martin, D., Marx, M.C., Hansen, H., Mourier, A., Nemazanyy, I. et al. (2017) CLUH regulates mitochondrial metabolism by controlling translation and decay of target mRNAs. *The Journal of Cell Biology*, **216**, 675–693.

Scheer, H., de Almeida, C., Ferrier, E., Simonnot, Q., Poirier, L., Pflieger, D. et al. (2021) The TUTase URT1 connects decapping activators and prevents the accumulation of excessively deadenylated mRNAs to avoid siRNA biogenesis. *Nature Communications*, **12**, 1298.

Sen, A. & Cox, R.T. (2016) Clueless is a conserved ribonucleoprotein that binds the ribosome at the mitochondrial outer membrane. *Biology Open*, **5**, 195–203.

Senkler, J., Senkler, M., Eubel, H., Hildebrandt, T., Lengwenus, C., Schertl, P. et al. (2017) The mitochondrial complexome of Arabidopsis thaliana. *The Plant Journal*, **89**, 1079–1092.

Tomal, A., Kwasniak-Owczarek, M. & Janska, H. (2019) An update on mitochondrial ribosome biology: the plant mitoribosome in the spotlight. *Cell*, **8**, 1562.

Vardi-Oknin, D. & Arava, Y. (2019) Characterization of factors involved in localized translation near mitochondria by ribosome-proximity labeling. *Frontiers in Cell and Development Biology*, **7**, 305.

Vellosillo, T., Aguilera, V., Marcos, R., Bartsch, M., Vicente, J., Cascon, T. et al. (2013) Defense activated by 9-lipoxygenase-derived oxylipins requires specific mitochondrial proteins. *Plant Physiology*, **161**, 617–627.

Vincent, T., Vingadassalon, A., Ubrig, E., Azeredo, K., Srour, O., Cognat, V. et al. (2017) A genome-scale analysis of mRNAs targeting to plant mitochondria: upstream AUGs in 5′ untranslated regions reduce mitochondrial association. *The Plant Journal*, **92**, 1132–1142.

Waltz, F. & Giege, P. (2020) Striking diversity of mitochondria-specific translation processes across eukaryotes. *Trends in Biochemical Sciences*, **45**, 149–162.

Waltz, F., Nguyen, T.T., Arrive, M., Bochler, A., Chicher, J., Hammann, P. et al. (2019) Small is big in Arabidopsis mitochondrial ribosome. *Nature Plants*, **5**, 106–117.

Welchen, E., Garcia, L., Mansilla, N. & Gonzalez, D.H. (2014) Coordination of plant mitochondrial biogenesis: keeping pace with cellular requirements. *Frontiers in Plant Science*, **4**, 551.

Williams, C.C., Jan, C.H. & Weissman, J.S. (2014) Targeting and plasticity of mitochondrial proteins revealed by proximity-specific ribosome profiling. *Science*, **346**, 748–751.

Xu, J. & Chua, N.H. (2011) Processing bodies and plant development. *Current Opinion in Plant Biology*, **14**, 88–93.

Zanetti, M.E., Chang, I.F., Gong, F., Galbraith, D.W. & Bailey-Serres, J. (2005) Immunopurification of polyribosomal complexes of Arabidopsis for global analysis of gene expression. *Plant Physiology*, **138**, 624–635.

Zhang, Y., Chen, Y., Gucek, M. & Xu, H. (2016) The mitochondrial outer membrane protein MDI promotes local protein synthesis and mtDNA replication. *The EMBO Journal*, **35**, 1045–1057.